Key Techniques of Prevention and Control for Reservoir Landslides Based on Evolutionary Process

Huiming Tang, Liangqing Wang, Changdong Li, and Zongxing Zou

Abstract

The essence of reservoir landslide treatment is to change its evolution process. It is hard to guarantee the effectiveness and safety of the landslide prevention and control technology that ignores the evolution processes. Guided by the thought of evolution, this study introduced some key techniques of reservoir landslide prevention and control. Seven evolution modes are summarized for rock slides and the optimal control measures suitable for each evolution mode and different evolution stages are suggested. The dynamic stability evaluation method is proposed considering the evolution process of the slip zone soil strength. This study introduces the methods for determining optimal pile positions for step-shaped sliding surfaces, the optimal plane arrangement of stabilizing piles, and their reasonable embedded lengths. Finally, two demonstration bases for comprehensive prevention and control of large reservoir landslides that were established in the Three Gorges Reservoir area (TGRA) were introduced, which is of great scientific and application value to the improvement of reservoir landslide prevention and control techniques.

Keywords

Reservoir landslide • Landslide prevention and control • Evolution process • Demonstration base

1 Introduction

Landslide, one of the world's major geohazards, are often accompanied by huge social and economic losses and poses a great threat to human lives as well as sustainable development. Water is one of the main driving factors of landslide evolution, especially for those located in reservoir areas (Zhang et al. 2021). The hydrogeological conditions have undergone significant and continuous changes under the impact of the long-term fluctuation of reservoir water level and seasonal rainfall, which increased the difficulty of reservoir landslide prevention and control. For instance, since the first impoundment in 2003, a total of 4256 large-scale landslides have been identified in the world-renowned Three Gorges Reservoir area (TGRA), costing the government up to 100 billion RMB in the treatment, yet many challenges remained (Tang et al. 2019). Reservoir landslide has become an important factor threatening the safety of waterborne transport and engineering construction in reservoir areas, and it is urgent to carry out in-depth research on its prevention and control.

Deficiencies still exist in the current research on reservoir landslide prevention and control. On the one hand, reservoir landslides have the basic characteristic of evolution, which is accompanied by different evolution modes and evolution stages that are highly related to the landslide's structural development, deformation failure patterns, and deterioration law of physical and mechanical parameters. The design of reservoir landslide control measures that ignore these factors fails to fully consider the synergistic effect of the landslide-control-structure system, which makes it difficult to guarantee its control effect and long-term stability of

H. Tang (✉) · L. Wang
Faculty of Engineering, China University of Geosciences, Wuhan, 430074, Hubei, China
e-mail: tanghm@cug.edu.cn

L. Wang
e-mail: wangliangqing@cug.edu.cn

C. Li · Z. Zou
Badong National Observation and Research Station of Geohazards, China University of Geosciences, Wuhan, 430074, China
e-mail: lichangdong@cug.edu.cn

Z. Zou
e-mail: zouzongxing@cug.edu.cn

© The Author(s) 2023

I. Alcántara-Ayala et al. (eds.), *Progress in Landslide Research and Technology, Volume 1 Issue 2, 2022*, Progress in Landslide Research and Technology,
https://doi.org/10.1007/978-3-031-18471-0_2

landslide. On the other hand, although institutions worldwide have attached great importance to the role of large in-situ test bases in geohazard research, few relevant demonstration bases have been built in the field of reservoir landslide prevention and control. Therefore, it is essential to carry out the study on reservoir landslide prevention and control techniques based on evolutionary processes and construct relevant demonstration bases.

2 Evolution Modes of Reservoir Landslide

By analyzing the geological structure, development pattern, evolutionary characteristics, and evolutionary process of reservoir landslides, seven types of rock landslide evolution modes are summarized as shown in Fig. 1. Seven evolution mode include progressive slip along gentle-dip layer I, progressive slip along gentle-dip layer II, bucking failure along steep-dip layer, creep slip along deep layer, plastic flow slip of weak interlayer, breakthrough abrupt slip in inclined cross-cutting layer and toppling failure in steep anti-dip layer. Each of the above evolution modes is divided into three evolutionary stages, and the corresponding evolutionary features of each evolutionary stages are described as follows.

For the mode of progressive slip along gentle-dip layer I (Fig. 1a), vertical tension cracks appear on the surface of the slope's frontal part under the manual excavation or river cutting in its stage I, named the leading edge unloading rebound stage. Then, in the crack extension stage (stage II), surface water seeps in along these cracks and accelerate the process of erosion or dissolution, so the cracks continue to expand in depth, which causes a new unloading effect on the rock mass behind the cracks, forming multiple sets of parallel tension cracks. Eventually, in the sliding surface penetration damage stage (stage III), the sliding mass keeps creeping until the mechanical properties of the slip zone are weakened to fail to balance the sliding force.

Different from the previous mode, progressive slip along gentle-dip layer II's cracks develop from the trailing edge to the leading edge of the landslide (Fig. 1b). In stage I, also called the trailing edge tension fracture formation stage, the crack is formed under the joint effect of the tensile stress and surface water at the trailing edge of the landslide. In stage II, (crack extension stage), the cracks develop from the surface to the deep until the underlying weak interlayer of the landslide is cut. In stage III (sliding surface penetration damage stage), the weak layer or sliding zone of the landslide is further softened and cracks expand into the trenches under the continuous effect of rainfall and gravity. When heavy rainfall continues in the landslide area, the sliding surface gradually penetrates, and the trailing edge fissure water provides lateral gradient force. Once the sliding force of the upper rock mass exceeds the resistance force providing by the sliding surface, the landslide occurs.

In stage I of bucking failure along steep-dip layer mode (Fig. 1c), also called the slight bending and deformation stage, the buoyancy between rock layers gradually increases and the shear strength of weak layer gradually decreases under the effect of rainfall and groundwater. Affected by this, the stratum of the landslide's shallow surface of the upper part began to creep, and the lower part is squeezed under gravity. In the creeping and squeezing, the trailing edge rock starts cracking and bending at the slope toe. During this process, the landslide comes to stage II (bending bulge loosening stage), and the interlaminar dislocation of the landslide shallow stratum gets increasingly intense. It led to the formation of a tension collapse zone at the trailing edge and a bending shape with a tension fracture zone at the toe of the landslide. Finally, with the gradual penetration of the tension fracture zone and the gradual enlargement of the tension collapse zone, the leading edge of the landslide slides out along the tension fracture zone and the rock stratum at the trailing edge slides along the sliding surface, that is, collapse slip stage (stage III).

The creep slip along deep layer mode includes three stages: deep slip zone formation stage (stage I), creep-slip stage (stage II), and start-slip destabilization stage (stage III) (Fig. 1d). During stage I, various factors such as gravity, tectonic movement, river undercutting and rainfall make the deep shear stresses of unstable slopes develop and concentrate, and then the creep shearing occurs locally. Further, in the stage II, some shear creeping surface are gradually penetrated from the local to the whole affected by gravity, rainfall, and other external loads. Finally, affected by the river erosion and water level fluctuation, deformation and failure occur in the location of steep terrain with groundwater retention, and even overall sliding failure.

As shown in Fig. 1e, the evolution stages of plastic flow slip of weak interlayer mode differ significantly. In the trailing edge crack formation stage (stage I), the deep weak layer flows to the free face affected by various external factors, causing tensile stress in the middle and rear part of the landslide. Cracks begin to appear under tensile stress and gradually increase and deepen with the continuous plastic flow of the landslide. In the subsequent crack extension stage (stage II), the sliding mass moves along the weak structural plane as a whole with the tension cracks developed. The sliding mass disintegrates under differentiated plastic flow developed in the uneven weak layer. Finally, the sliding zone expends laterally driven by the finest path of shear stress elimination. The expending process is terminated by its slipping-off separation in the overall slip disintegration stage (stage III).

At the beginning of breakthrough abrupt slip in inclined cross-cutting layer mode, affected by tectonic stress and

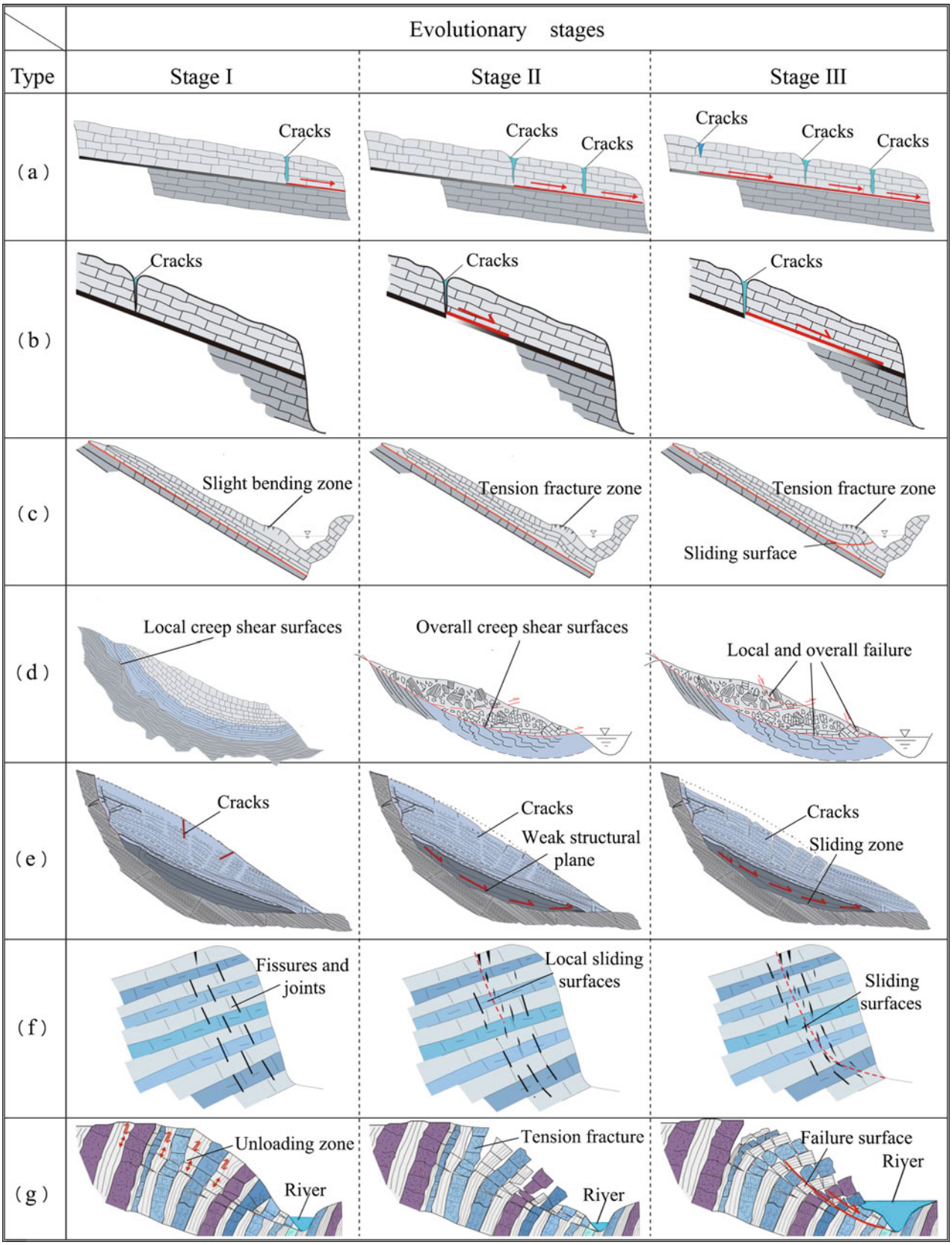

Fig. 1 Seven evolution types and stages of reservoir rock landslide

unloading rebound effect, initial fissures and joints develop in the shallow surface layer parallel to the slope surface, which is summarized as the intra-layer tensile fracture formation stage (stage I) (Fig. 1f). Under internal and external effects, the strength of the rock mass continues to decrease. Therefore, the tension fracture continues to expand and the local sliding surfaces start connecting, which is called the tension fracture development stage (stage II). With the continuous expansion of tension fracture, the sliding surface continues to develop towards the slope toe. When the sliding surface is totally formed, the whole rock mass falls, which is the cut layer fracture penetration stage (stage III).

For the toppling failure in steep anti-dip layer mode (Fig. 1g), initial toppling is its stage I, where, the rock mass undergoes interlayer shear movement due to a strong unloading rebound. Then, a certain depth of unloading zone is formed near the surface of the landslide, where the tension fracture is developed. The rock stratum begins to bend extensively towards the free surface and the tension fracture or tension deformation developed along the existing transverse joints, results in further segmentation of the rock column. Subsequently, the intact rock column is divided into several short rock columns by the new tension fracture and the existing transverse joints. The slope enters the self-stabilizing creep stage (stage II), in which the rock mass deforms at a low rate. With the rise of water level, a unified tension shear fracture surface is formed in the front part of the slope and shear slip occurs. The steep failure surface develops in depth and finally intersects with this tension shear fracture surface in front of the slope. Then, an interconnected shear surface is formed and results in an overall slicing slip, that is, the formation of unified shear surface and failure stage (stage III).

3 Suitability of Reservoir Landslide Control Measures Based on the Evolution Process

The evolution mechanism is an important aspect in the study of reservoir landslides. Most of the reservoir landslides are nurtured by tectonic dynamics and river valley dynamics, then evolve due to human engineering construction, and finally occur under the action of disaster-causing factors such as earthquakes, rainfall and reservoir water. During the evolution process, the landslide constantly undergoes structural changes and parameter deterioration, resulting in different forms of deformation and failure. The essence of reservoir landslide control is to change its evolution process. The effectiveness and long-term safety of reservoir landslide control measures that ignore this process are hard to guarantee. According to the division of seven reservoir landslide evolution modes and corresponding evolution stages, the specific control measures suitable for reservoir landslides in different evolution stages are suggested in Table 1. These measures have been successfully employed in the landslide management of the TGRA and have achieved satisfactory results.

Hongshibao landslide is a typical landslide management demonstration project in the TGRA that considered the landslide evolution process (Tang et al. 2019). Hongshibao landslide area is about 600 m long from north to south, higher in the south and lower in the north, with an elevation of 270–70 m and a width of about 500 m from east to west. Due to the characteristics of landslide evolution, various engineering countermeasures were used to reinforce the slope, including slope reduction and load shedding for the suitable slope position, setting retaining walls to improve the shallow stability and the arranging stabilizing piles in the slope. As shown in Fig. 2, the most effective protective measures are cantilever piles and anchor piles. Two rows of anti-slip piles were arranged to solve the problem of deep and shallow anti-slip stability of the site slope, and also to solve the slope stability problem caused by the reservoir water level changes sharply between 175 and 145 m. Based on the monitoring and observations reported, the above control measures have an effective and obvious control effect on the Hongshibao landslide.

4 Evaluation of Reservoir Landslide Dynamic Stability

With the evolution of landslides, the stability of landslides constantly evolves and develops, which is a dynamic process. Therefore, dynamic stability evaluation is required to evaluate the stability state of landslides.

Dynamic Stability Evaluation Method

In the evaluation of landslide stability, a dynamic stability evaluation method is proposed considering the evolution process of the slip zone soil strength. Firstly, the constitutive model and shear strength evolution model are developed for describing the relation between shear stress and shear displacement, and the relation between shear strength and shear displacement, respectively.

The strength properties are evolving during the process of the deformation and failure of slip zone soil, and the process is of continuous damage (Yan et al. 2022). From the aspect of damage theory, soil damage is regarded as a process of accumulation of plastic deformation in the soil and weakening of soil strength. Consequently, soil can be divided into two parts Fig. 3a: a damaged part and an undamaged part (or intact part). So, based on the Lemaitre strain equivalence hypothesis, the shear strength of slip zone soil can be formulated by,

Table 1 Recommended reservoir landslide control measures based on evolution process

Type	Evolution mode	Structural characteristics	Evolution stages		Recommended control measures
(a)	Progressive slip along gentle-dip layer I	① Gentle dip angle bedding rock structure; ② Medium to thick hard rocks; ③ Horizontal bedding plane	Stage I	Leading edge unloading rebound	Surface drainage
			Stage II	Crack extension	Surface drainage and the certain support measures in leading edge
			Stage III	Sliding surface penetration damage	Anchor cable support can be set when the slope is steep, and stabilizing piles combined with corresponding drainage measures can be set when the slope is gentle
(b)	Progressive slip along gentle-dip layer II	① Gentle dip angle bedding rock structure; ② Medium to thick hard rocks; ③ Horizontal bedding plane	Stage I	Trailing edge tension fracture formation	Surface and underground drainage
			Stage II	Crack extension	Surface and underground drainage, slope excavation and load shedding in the rear part
			Stage III	Sliding surface penetration damage	The combination of slope excavation and load shedding and prestressed anchor cables setting, supplemented by corresponding drainage measures
(c)	Bucking failure along steep-dip layer	① Steep dip angle bedding rock structure; ② Thin to medium bedding rock stratum; ③ Horizontal bedding plane	Stage I	Slight bending and deformation	Surface drainage
			Stage II	Bending bulge loosening	Surface and underground drainage, and slope toe pressed and backfilled if necessary
			Stage III	Collapse slip	Slope excavation and load shedding in the rear part, stabilizing pile set in the front part and supplemented by corresponding drainage measures
(d)	Creep slip along deep layer	① Steep dip angle in the upper part and gentle dip angle in the lower part bedding rock structure; ② Concave bending bedding plane	Stage I	Formation of deep sliding zone	Surface and underground drainage
			Stage II	Creep-slip	Underground drainage and supplemented by real-time monitoring of slope surface and deep slope displacement
			Stage III	Start-slip destabilization	Relocate residents if landslide is very large
(e)	Plastic flow slip of weak interlayer	① Bedding rock structure or quasi-homogeneous rock mass; ② Soft plastic belt under sliding mass	Stage I	Trailing edge crack formation	Surface and underground drainage
			Stage II	Crack extension	Drainage is the main concern, and anti-slip piles should be set at the front edge of the slope
			Stage III	Overall slip disintegration	Drainage and front support protection. Relocate residents if landslide is very large
(f)	Breakthrough abrupt slip in inclined cross-cutting layer	① Steep anti-dip bedding rock structure; ② Thin to medium bedding rock stratum; ③ Slight toppling bedding plane	Stage I	Intra-layer tensile fracture formation	Surface drainage
			Stage II	Tension fracture development	Surface and underground drainage, the front part is supplemented by certain support measures
			Stage III	Cut layer fracture penetration	Anchor cable support
(g)	Toppling failure in steep anti-dip layer	① Steep anti-dip bedding rock structure; ② Thin to medium bedding rock stratum; ③ Toppling bedding plane	Stage I	Initial toppling	Surface drainage
			Stage II	Self-stabilizing creep	Drainage, real-time monitoring of landslide
			Stage III	Formation of unified shear surface and failure	Prestressed anchor cable support, and backfill pressure monitoring in the leading edge

$$\tau = K_s u(1 - D) + \tau_r D \tag{1}$$

where τ represents the shear stress in the microelement; u is the shear displacement; the damage degree D is a physical value reflecting the evolution process, which varies with the shear deformation of the soil, ranging from 0 to 1. K_s as the shear stiffness with a unit of kPa/mm, the slope of linear deformation stage in Fig. 3b. τ_r is the residual strength of the damage part, see in Fig. 3c.

The damage degree directly reflects the evolution of shear stress in the slip zone soil, and it can be solved from the perspective of statistical damage theory. So, it is assumed that the microelement strength of the slip zone soil obeys Weibull probability distribution in the process of shear damage:

$$p(x) = \frac{m}{u_0}\left(\frac{x}{u_0}\right)^{m-1} exp\left[-\left(\frac{x}{u_0}\right)^m\right] \tag{2}$$

Thus, the shear stress evolution equation of the slip soil is obtained as follows:

$$\tau = \begin{cases} K_s u, \ (u < u_y) \\ K_s u\left\{exp\left[-\left(\frac{u-u_y}{u_0}\right)^m\right]\right\} \\ + \tau_r\left\{1 - exp\left[-\left(\frac{u-u_y}{u_0}\right)^m\right]\right\}, (u \geq u_y) \end{cases} \tag{3}$$

where the parameters K_s, u_y and τ_r can be obtained by shear stress-shear displacement curve. The parameters u_0 and m in the model can also be further determined based on the properties of the curve. When the soil shear deformation is before the yield point, only elastic deformation occurs, that is $u < u_y$; when the soil deformation exceeds the yield point, the damage occurs in the soil, that is $u \geq u_y$.

Meanwhile, by adopting the property of peak point of τ–u curve, the model parameter u_0 and m can be solved as,

$$m = \frac{K_s(u_p - u_y)}{(K_s u_p - \tau_r) ln\left(\frac{K_s u_p - \tau_r}{\tau_p - \tau_r}\right)}, \ u_0 = \frac{u_p - u_y}{\sqrt[m]{ln\left(\frac{K_s u_p - \tau_r}{\tau_p - \tau_r}\right)}} \tag{4}$$

where u_p and τ_p are the shear displacement and shear stress corresponding to the peak point of the τ–u curve, respectively, in this peak point, it requires $\frac{\partial \tau}{\partial u}\Big|_{u=u_p} = 0, \tau|_{u=u_p} = \tau_p$.

Based on the shear constative model and the linear relation between the model parameters and the normal stress, the evolution model of shear strength τ_s with the shear placements is expressed as (Fig. 4),

$$\tau_s = \begin{cases} \tau_p, \ (u < u_p) \\ K_s u\left\{exp\left[-\left(\frac{u-u_y}{u_0}\right)^m\right]\right\} \\ + \tau_r\left\{1 - exp\left[-\left(\frac{u-u_y}{u_0}\right)^m\right]\right\}, (u \geq u_p) \end{cases} \tag{5}$$

The shear strength of the slip zone soil evolves with the displacement, which leads to the stability factor of landslide evolves with the displacement. According to the force balance condition of the landslide slice along the sliding surface direction (Fig. 5), the residual thrust P_i of slice i based on the strength reduction method is as follows:

$$P_i = P_{i-1}\cos(\alpha_{i-1} - \alpha_i) + T_i - R_i/F_r \tag{6}$$

where P_{i-1} represents the residual thrust of slice $i - 1$; α_{i-1} and α_i are the inclination angles of the sliding surface at slice $i - 1$ and slice i, respectively, for the anti-warping part of the landslide, the value is negative; T_i represents the sliding component of the gravity of the slice i, $T_i = W_i \sin\alpha_i$; R_i is the anti-sliding force of slice i,$R_i = \tau_i l_i$; τ_i represents the shear strength provided by the slip zone at the slice i, which can be calculated by the shear constitutive model; F_r is the overall strength reduction factor.

Based on the equilibrium analysis of forces at the slice i in the direction perpendicular to the sliding surface, the normal stress σ_{ni} is formulated by,

$$\sigma_{ni} = \frac{P_{i-1}\ sin(\alpha_{i-1} - \alpha_i) + W_i'\ cos\,\alpha_i}{l_i} \tag{7}$$

where W_i' is the effective gravity of slice i, $W_i' = W_{1i}' + W_{2i}'$, and W_{2i}' is the effective gravity of the part of slice i below the groundwater level, that is, the effective gravity of the soil below the water level is used to calculate the anti-sliding force regardless of whether there is a stable seepage field or not.

Then, under the condition of the preset strength reduction factor F_r, calculate the residual thrust P_n by one from the first slice at the rear edge of the landslide by Eq. 6. When the landslide is in a critical state, that is limit equilibrium state, the strength reduction factor F_r in this state is defined as the stability factor F_s of the landslide. Since the Eq. 6 for solving the residual thrust contains the shear strength τ_i, which is an exponential function obtained from the shear constitutive model (Eq. 5). In the shear constitutive model, all parameters are related to the normal stress σ_{ni}, so the evolution of shear strength τ_i with displacement u is related to the normal stress σ_{ni}, and each landslide slice has different normal stress. Therefore, the solution of landslide stability factor is a highly nonlinear problem with an analytical expression of stability factor, which can only be calculated by an iterative method. The detailed flow of the landslide dynamic stability evaluation method is shown in Fig. 6.

The Case Study of Outang Landslide

The Outang landslide, a typical large deep bedding bedrock landslide in TGRA, is located in Anping Town, Fengjie

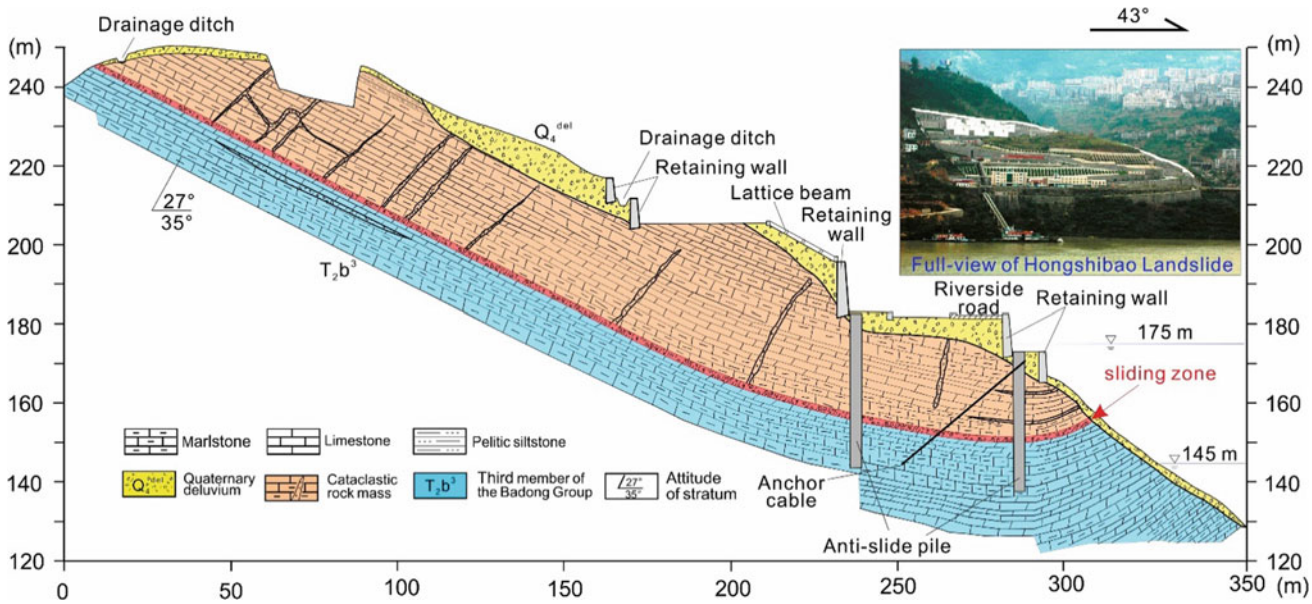

Fig. 2 Cross section of the Hongshibao landslide, whose toe is affected by fluctuations of the TGR level. Drainage ditches, retaining walls, lattice beams and stabilizing piles were constructed to stabilize this actively creeping landslide (Tang et al. 2019)

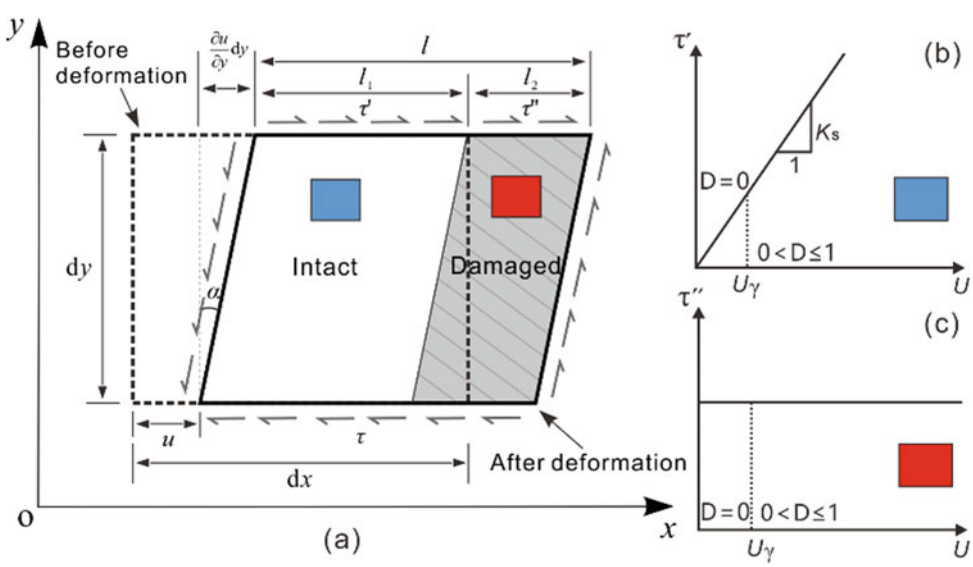

Fig. 3 The microelement damage mechanics model of the slip soil during shear process (Yan et al. 2022)

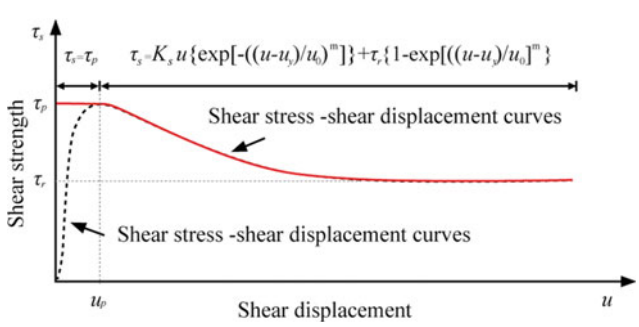

Fig. 4 The τ–u and τ_r–u curves of slip zone soil (Yan et al. 2022)

County, Chongqing City. The landslide is 1990 m long in the N–S longitudinal direction and 899 m wide in the E–W transverse direction, with a total area of 1.769 million m^2 and a total volume of 89.5 million m^3. The landslide is composed of Slide 1, Slide 2 and Slide 3 (Fig. 7a and b), the front elevation of the landslide is 90–102 m, and the rear elevation is 705 m. The slip zone soil is mainly the argillization product of carbonaceous claystone and carbonaceous shale, which is black and gray black, with high clay content, luster and good toughness (Fig. 7c and d).

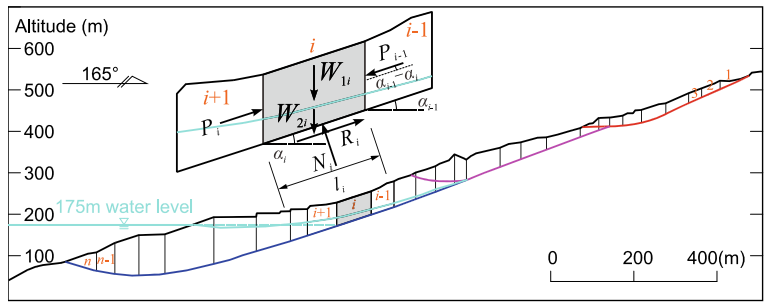

Fig. 5 Force analysis of the slices of a landslide (Yan et al. 2022)

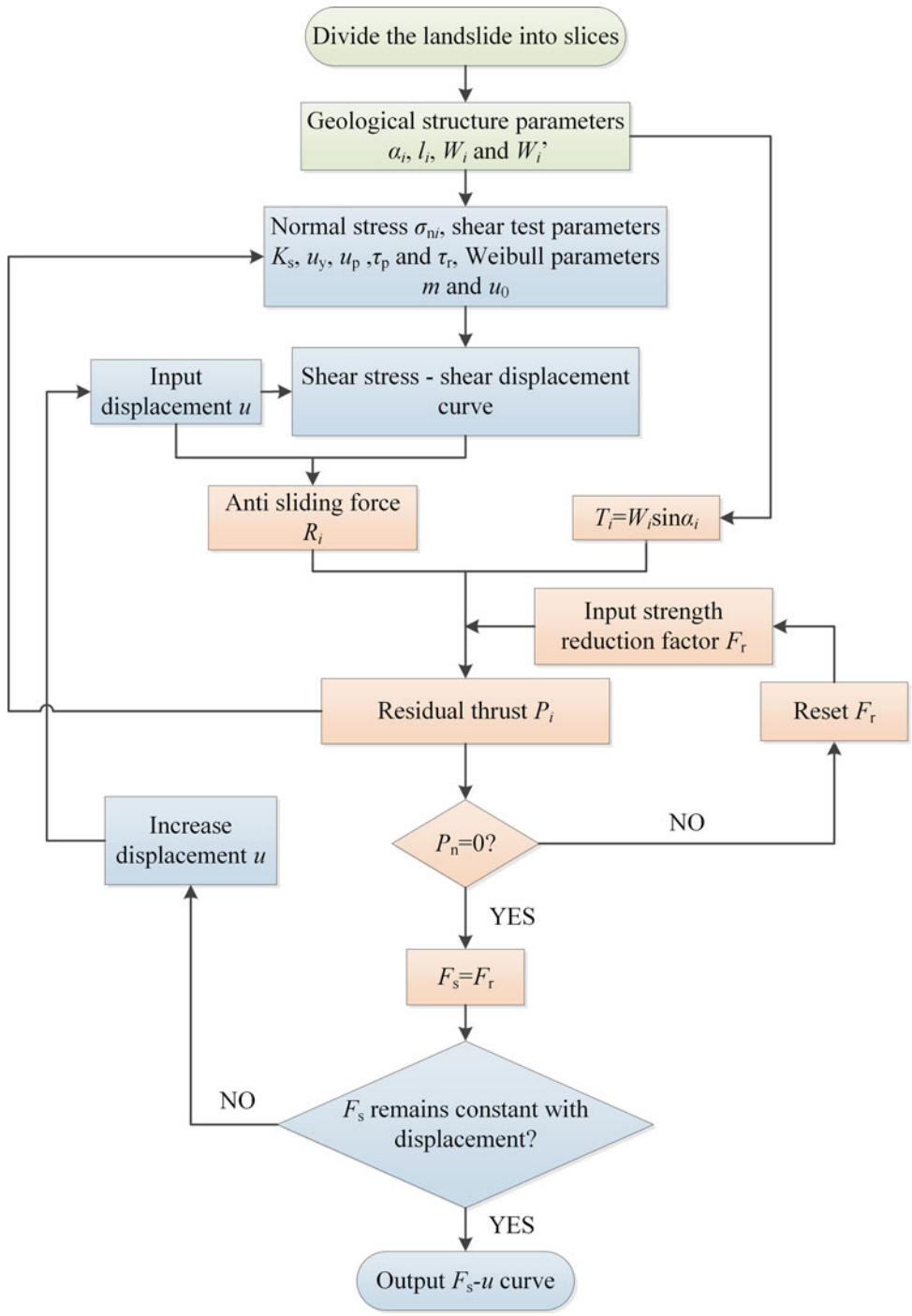

Fig. 6 Flow of landslide dynamic stability evaluation method (Yan et al. 2022)

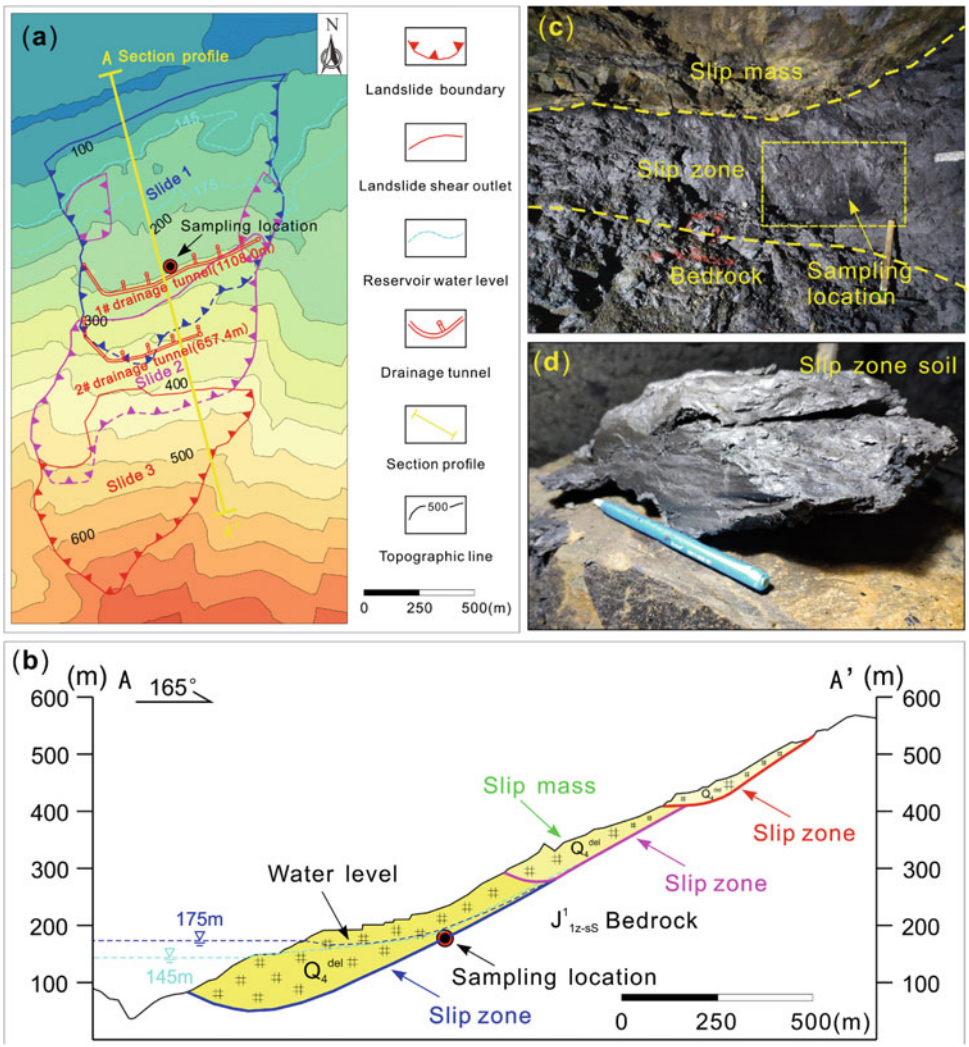

Fig. 7 **a** the plain view of the landslide; **b** the main section of the landslide; **c** the overall view of the landslide; **d** the slip zone of the landslide (Yan et al. 2022)

The stability evolution of Outang landslide without considering groundwater condition and 175 m water level condition is analyzed respectively. From Fig. 8, it shows that with the increase of landslide displacement, the landslide stability factor decreases at a gradually decreasing attenuation rate, and the stability factor tends to a constant value under large displacement, which is consistent with the strain softening phenomenon of the slip zone soil: the shear strength gradually decreases with displacement and tends to be constant until reaching the residual strength stage. It also shows that the displacement required for a constant stability factor is greater than the displacement required for the slip zone soil to reach the residual strength stage. It is attributed to that the Outang landslide is a deep giant landslide, and the normal stress of the slip zone is high stress, up to 2000 kPa, the strain softening phenomenon of the sip zone soil is less obvious under large normal stress, and the displacement required to decay from peak strength to residual strength increases.

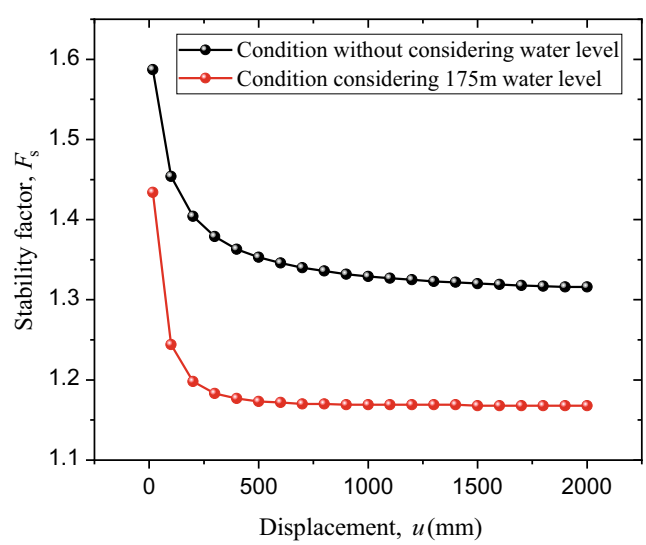

Fig. 8 Stability evolution characteristics of Outang landslide (Yan et al. 2022)

Without considering the reservoir water level, the stability factor of Outang landslide gradually decreases from 1.587 to 1.316 and remains constant, indicating that the landslide deformation has a significant impact on the stability of the landslide. Under the condition of 175 m reservoir water level, the landslide stability factor gradually evolves from 1.434 to 1.168, and then remains constant. Comparing the stability of the landslide with or without considering the reservoir water, it is concluded that the reservoir water has a significant impact on the stability of Outang landslide, and the attenuation amplitude of the peak stability factor with the water level ΔF_{s-w} is 0.153, and the attenuation amplitude of residual stability factor with the water level ΔF_{s-w} is 0.148. The main reason for the effect of reservoir water on landslide stability is that the reservoir water causes the reduction of the effective gravity of the anti-sliding section of the landslide. The front part of the Outang landslide has a small inclination angle and even an inverted section, which is the main anti-sliding section. Affected by the reservoir water, the effective gravity of the anti-sliding section decreases, resulting in the reduction of the effective normal stress and anti-sliding force of the landslide, which leads to the reduction in the landslide stability factor. Therefore, the drainage engineering is a feasible measure for preventing and controlling large-scale landslides.

5 Key Techniques of Reservoir Landslide Prevention and Control

Determination of Optimal Pile Position for Landslide with Step-shaped Sliding Surface

Previous determinations of the optimal stabilizing pile location have generally been based on the idealized assumption of arc-shaped sliding surfaces. This assumption, however, may involve considerable error especially for the identified numerous colluvial landslides located in the TGRA of China that have step-shaped sliding surfaces. To address the problem, a strategy, termed the local safety partitioning (LSP) methodology, for accurately determining optimal pile locations for step-shaped configurations. Instead of assuming the sliding surface to be arc-shaped, this strategy considers the actual sliding shapes.

The LSP methodology contains a framework of several implantation steps, in which the Swedish slice method is initially employed to calculate the local safety factors of each soil slice above the sliding surface; then, several landslide mass partitions are identified as high-safety partitions and low-safety partitions, and finally the stabilizing pile is placed between high-safety masses and low-safety masses, as schematized in Fig. 9.

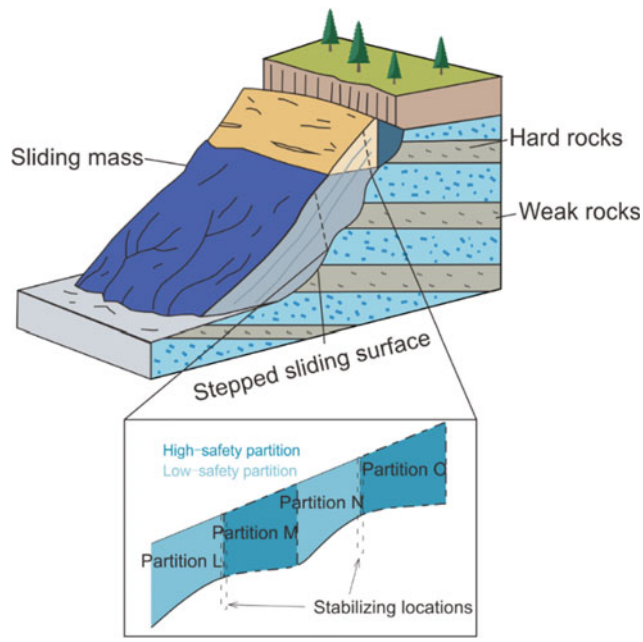

Fig. 9 Schematic diagram for the landslide with stepped sliding surface and local partitions of high and low safety (Tan et al. 2018)

The LSP methodology basically contains four sequential calculation steps:

(i) Divide the landslide mass into slices, designated I in Fig. 10. For each slice we generally require the bottom brim to be a straight line, thus a careful slicing should be conducted. This is in line with the Swedish slice method.

(ii) Acquire the K_{Li} of every individual slice, then draw the local safety-slice number curve to find out the mutational points on the curve. Procedures for identifying the mutational points would be executed including: first calculate out the slopes of every adjacent two K_{Li} values, next make subtraction of two adjacent slopes and acquire the slope subtraction values, then identify the biggest value of slope subtraction. Thus, the mutational point corresponds to the mid slice of the three subsequent slices. For example, slices 5, 6 and slices 6, 7 in Fig. 10 have the biggest slope subtraction, then slice 6 corresponds to the mutational point on the curve. Further, when the K_{Li}—slice number curve has more than one inflection, the procedure should be repeated around each inflection until all the mutational points are identified.

(iii) Identify partitions by mutational slices (slices covering mutational points) as denoted by III in Fig. 10, then calculate the local safety factor (K_L) of each

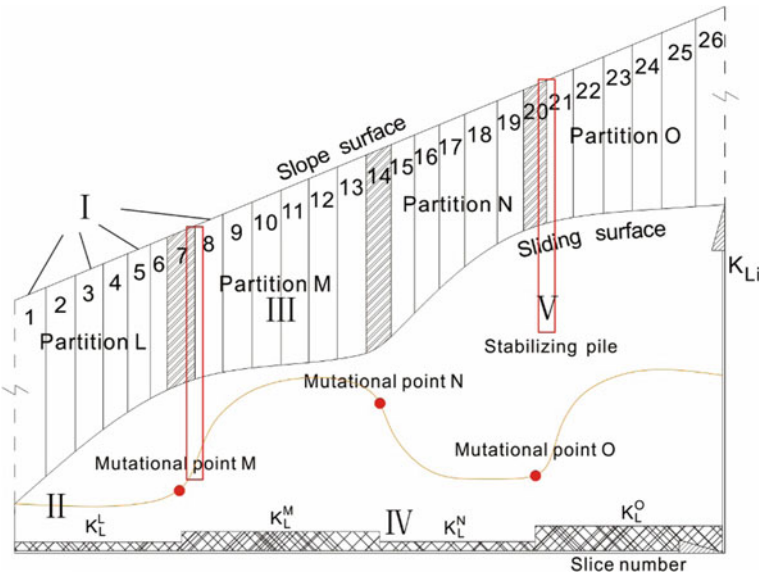

Fig. 10 Schematic diagram for the implementation of the LSP methodology. It is introduced to explain step (i) to (iv) for an explicit demonstration (Tan et al. 2018)

partition (IV in Fig. 10). For this step, adjacent two mutational slices would be identified as the two boundaries of the local partition. As illustrated in Fig. 10, the K_{Li}—slice number curve has three mutational points, denoting the mutational slice No. 7, 14 and 20. Then, four partitions were identified by the three slices, characterized by discriminating high and low K_L.

(iv) Put the stabilizing pile in between two partitions, where behind the pile (opposite to the sliding direction) contacts the partition with high K_L and in front the pile contacts the partition with low K_L.

The performance of the presented methodology is illustrated using the Jinle No. 2 landslide case for well-rounded demonstration and using the Yancun landslide case for additional validation. The results indicate that analysis of a reinforced landslide employing the LSP methodology acquires the largest factor of safety and smallest deflection, shear force and bending moment on the pile body compared with any other case from a series of positions which incorporating traditional positions for arc-shaped sliding surfaces. The presented methodology provides a simple but accurate determination of the optimal stabilizing pile location for stepped sliding surfaces, although it may involve errors and unexpected limitations when applied to arc shapes and peculiar scenarios.

Optimal Plane Arrangement Method of Stabilizing Piles

Among the current reinforcement structures, it is preferable to use the stabilizing piles to ensure safety of landslides, especially the large-scale colluvial landslides. Many colluvial landslides with pile improvement encouraged engineers to pay more attention on the design and effectiveness of stabilizing piles. With further studies on the landslides and stabilizing piles, more and more researchers have realized that landslide is a three-dimensional object rather than a two-dimensional profile, the conventional uniformly distributed driving force acting on the stabilizing piles should be replaced with the three-dimensional spatial distributed driving force in plane. Therefore, the engineers have to reconsider the corresponding issues related to the design of stabilizing piles, especially in the aspects of the pile spacing, stability of landslide and plane arrangement of piles. Though there are still several literatures that involve the soil arching effect, three-dimensional distribution characteristics of driving force and the concept of plane arrangement of stabilizing piles for colluvial landslides; unfortunately, only few of them can perform the quantitative studies on the whole optimal plane arrangement of stabilizing piles based on soil arching effect and the three-dimensional distributed driving force.

A novel optimal plane arrangement of stabilizing piles in terms of the provided half simplified flattened ellipsoid model, which can be used to describe the three-dimensional characteristics of sliding mass for colluvial landslides has been presented (see Fig. 11). By studying the friction soil arching effect between the adjacent stabilizing piles, a reasonable pile spacing model for stabilizing piles was deduced in consideration of the driving force and shear strength of sliding mass as well as the dimension of pile cross-section. Furthermore, the concept of stability limit was put forward to confine the rational arrangement region for stabilizing piles; consequently, the region beyond the rational arrangement region is not necessary to set piles anymore (see Fig. 12).

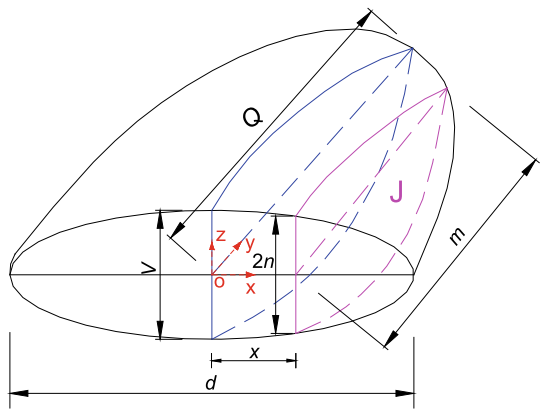

Fig. 11 Sketch of half flattened ellipsoid model for describing the spatial morphology of sliding mass for colluvial landslides. (V is the maximum depth of sliding mass, Q is the maximum horizontal distance from the pile to the crest, d is the width of landslide in the section along the pile-row, section J is the longitudinal profile with x distance to the major slip profile, $2n$ is the depth of sliding mass in section J, m is the distance along the oy axis direction in section J) (Li et al. 2015)

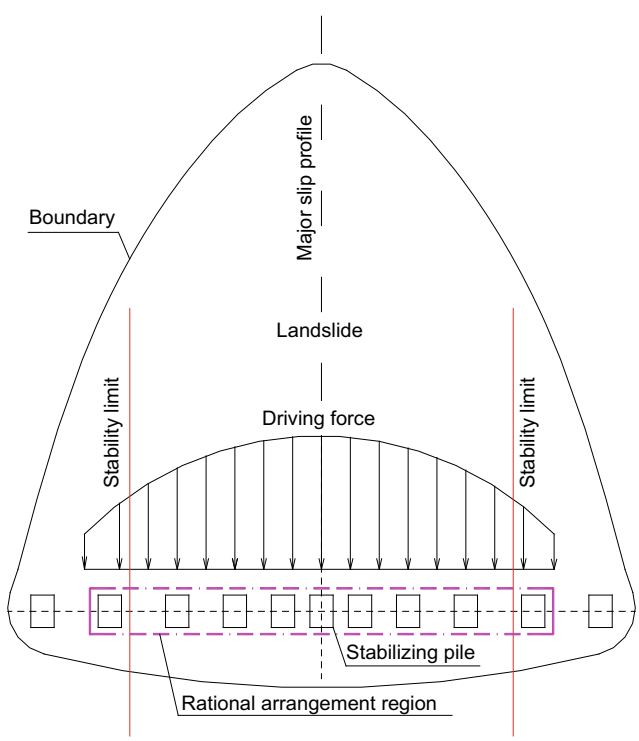

Fig. 12 Sketch of stability limit and rational arrangement region for stabilizing piles in a colluvial landslide (Li et al. 2015)

The friction soil arching effect was used to obtain the reasonable range of pile spacing. The corresponding calculation model can be utilized to determine the upper limit of the pile spacing because of the consideration merely on the effect of the friction soil arching. The solution of the reasonable net pile spacing S based on the friction soil arching can be obtained as (Li et al. 2015):

$$S = \frac{c \cdot a \cdot (2H + 1)}{q \cdot (1 - \tan\varphi) - \gamma \cdot H \cdot (\cos\theta \cdot \tan\varphi - \sin\theta)} \quad (8)$$

As stated above, the calculation model for net pile spacing (S) depends on the effect of the friction soil arching. Consequently, the pile spacing presented by Eq. 8 should be the maximum pile spacing. It is assumed that the total number of needed stabilizing piles is N, and any maximum net pile spacing S_i can be written as (Li et al. 2015):

$$S_i = \frac{c \cdot a \cdot (2H + 1)}{q_i \cdot (1 - \tan\varphi) - \gamma \cdot H \cdot (\cos \cdot \tan\varphi - \sin\theta)} \quad (9)$$

where q_i is the driving force intensity of the number i stabilizing pile along the ox direction, $i = 1, 2, \ldots, N$.

Erliban landslide located in Yichang City, China, was taken as an example to exhibit the optimal plane arrangement of stabilizing piles for colluvial landslides. Erliban landslide is a typical colluvial landslide located on the left bank of the Xiangxi River in Yichang City, China (Li et al. 2013). In view of the technical regulation of geological investigation and engineering design for landslide control in reservoir region of Three Gorges in Hubei Province (The head office for prevention and control of geohazards in the Three Gorge Reservoir Region of Hubei Province, 2003), the safety factor (F_s) of Erliban landslide should be 1.15, i.e., F_s = 1.15.

In the light of the definition of scale factor and the geometrical relationship, the position of stability limit of Erliban landslide can be obtained as X = 57.8 m in the XOY coordinate system presented in Fig. 14. Therefore, the stability coefficient of landslide is 1.02 in the major slip profile and is 1.15 at the stability limit section of X = 57.8 m (see Fig. 13). The blue curve with red dots shows the change trend of the stability coefficient of landslide from the major slip profile to the stability limit section.

Based on the confinement of rational arrangement region by the stability limit, the corresponding rational arrangement region for Erliban landslide can be determined by the bold magenta dash dot line in Fig. 13. Considering the impact of the pile length above the slip surface on pile spacing, an improved optimal non-uniformly spaced arrangement model was put forward. In view of the comparison between the conventional uniformly spaced arrangement and the improved optimal non-uniformly spaced arrangement, the improved optimal non-uniformly spaced arrangement method only requires 25 stabilizing piles rather than the 31 stabilizing piles in the conventional scheme, with an obtainable saving of 19.4% in the number of stabilizing piles (Li et al. 2015).

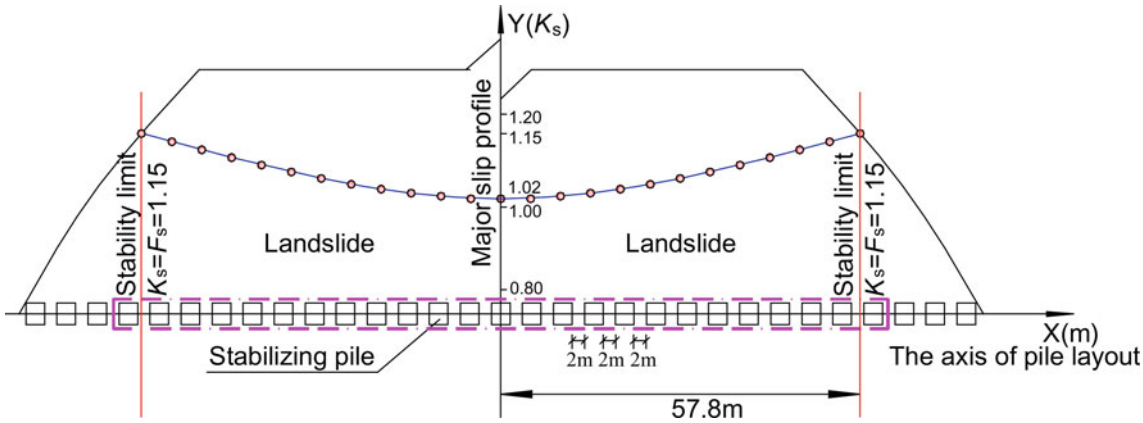

Fig. 13 Determination of the location of stability limit and rational arrangement region for Erliban landslide (Li et al. 2015)

Reasonable Embedded Length Determination Method of Stabilizing Piles

The reinforcement effect of landslides is influenced by the design parameters of stabilizing piles, especially the embedded depth has a great influence on the effect of stabilizing piles. For instance, the Jurassic strata are characterized by hard and weak interbedded rocks. Determining a reasonable embedded length is crucial to the design of piles that stabilize landslides. However, the presence of upper hard and lower weak bedrock presents a challenge when attempting to determine the reasonable embedded length of stabilizing piles. It is generally accepted that stabilizing piles can be set to stabilize a landslide. In engineering practice, strength design is always used to design stabilizing piles by focusing on bending moments and shear forces. However, pile deformation is rarely considered, especially when complex layered bedrock is present. Therefore, it is necessary to determine the reasonable embedded length of piles in bedrock with upper hard rock and lower weak rock based on the deformation control requirements set by industrial standards.

There is typically a negative power function relationship between the embedded ratio (ω) of a pile and the horizontal displacement of the pile head (xh) (Li et al. 2019), so the reasonable embedded ratio can be obtained if the allowable horizontal displacement of the pile head is known.

To better describe the embedded condition of the pile, an embedded pile ratio (ω) can be defined as the ratio between the embedded pile length and the total pile length. According to industrial standards (TB 10,025/J127; Standardization Administration of China 2006), the allowable degree of pile deformation ($x$hp) should be less than 1/100 of the pile length above the slip surface (h1), and it should also not exceed 10 cm. As pile head deflection is mainly dependent on the embedded length ratio of the pile (ω), the thickness of the upper hard rock layer in the bedrock (Th), the coefficient of subgrade reaction of the hard rock (Kh), the coefficient of subgrade reaction of the weak rock (Kw) (see Fig. 14), and the driving force per unit width behind the landslide (P), the horizontal displacement of the pile can be expressed as follows (Li et al. 2019):

$$\begin{cases} x_h = f(\omega,\ T_h,\ K_h,\ K_w,\ P) \\ x_{ha} \le 0.01h_1 \\ x_{ha} \le 10\ cm \end{cases} \tag{10}$$

Here, $x$ha is an upper limit on the horizontal displacement of the pile head. For a given landslide, h1, Th, Kh, Kw, and P can be determined. Consequently, due to the negative power function relationship between the embedded ratio and horizontal displacement (see Fig. 15), the reasonable embedded ratio (ωr) for piles can be expressed as below (Li et al. 2019):

$$\begin{cases} \omega_r = ax_{ha}^b \\ x_{ha} \le 0.01h_1 \\ x_{ha} \le 10\ cm \end{cases} \tag{11}$$

where a and b are undetermined constants that can be obtained from the completed work (Li et al. 2019).

The No.1 Majiagou landslide is approximately 540 m long and 200 m wide, approximately 9.7 km^2 in area and 1.3 million m^3 in volume, and has an average thickness of 12.7 m (Qinghai Province No. 906 Engineering Investigation and Design Institute 2006). The pile spacing (L) is 7.0 m. The total length of the stabilizing pile (**h**) is 22 m with a cantilever section length (**h_1**) of 14 m and an embedded section length (**h_2**) of 8 m. The current horizontal displacement of the pile head in the No. 1 landslide is roughly 15.0 cm. Assuming the presence of a lower weak rock layer, it is necessary to obtain the reasonable embedded length of the stabilizing pile to control pile deformation. In the original design scheme, the embedded length of pile (**h_2**) is 8 m. According to industrial standards (TB 10,025/J127,

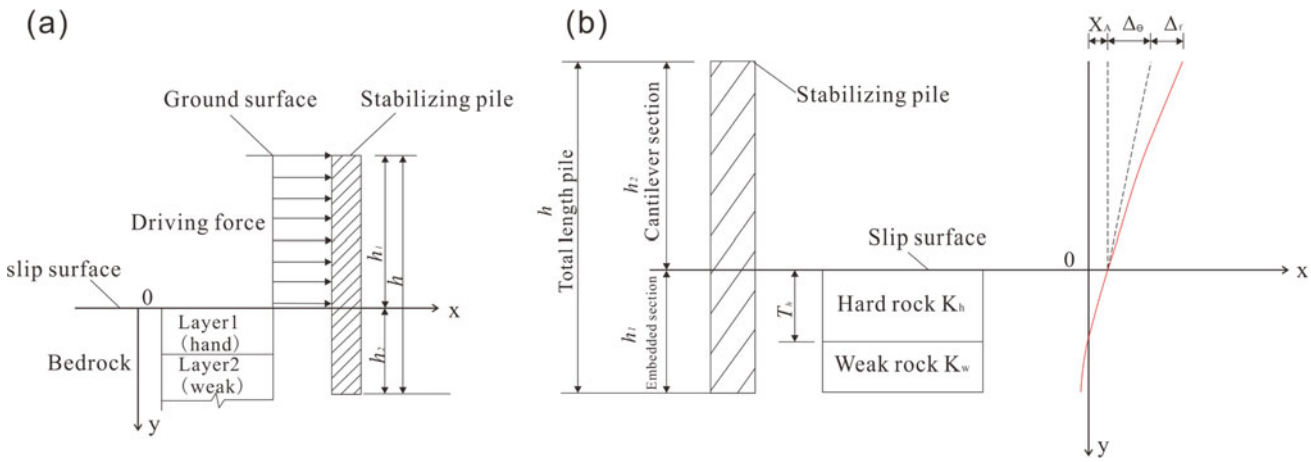

Fig. 14 Deformation calculation model of stabilizing pile in upper hard and lower weak bedrock; **a** sketch of a laterally loaded pile; **b** sketch of the deformation of a stabilizing pile subjected to the driving force of landslide (modified from Li et al. 2019)

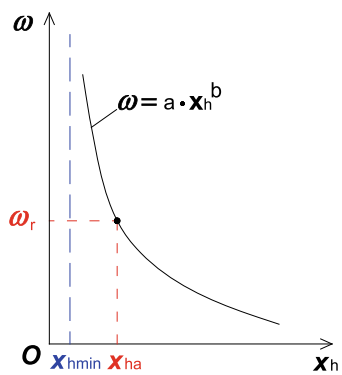

Fig. 15 Approach for determining the reasonable embedded ratio of a pile (Li et al. 2019)

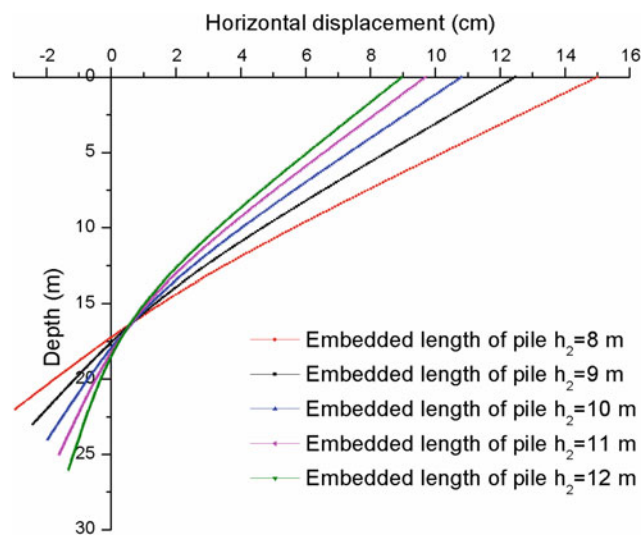

Fig. 16 Calculation results for pile deformations based on different embedded lengths (Li et al. 2019)

2006) and the second surveying and designing institute of the National Department of China Railway (1983), the recommended common embedded ratio of stabilizing piles ranges from 1/3 to 1/2. Consequently, to limit pile deformation, we consider embedded pile lengths (h_2) of 9, 10, 11, and 12 m. The calculated pile deformation levels found for these conditions are shown in Fig. 16 (Li et al. 2019).

Based on the assumption of an upper hard rock layer and a lower weak rock layer, the reasonable embedded length of piles for the Majiagou No. 1 landslide can be investigated in detail. By calculation by the above-mentioned model, it can be obtained that the reasonable embedded ratio (ω_r) of the piles is 0.435. Therefore, the corresponding reasonable embedded length (h_{2r}) of a pile is 10.8 m, i.e., the embedded length (h_{2r}) of a pile is at least 10.8 m to maintain pile head deformation within 10 cm as an industrial standard. According to the embedded ratios of stabilizing piles, the embedded ratio (ω) should increase from the current value of 0.364–0.435 to meet industrial standards. Therefore, the embedded ratio of stabilizing piles should be carefully considered during piles design due to its crucial influence on pile behavior (Li et al. 2019).

6 Demonstration Bases for Reservoir Landslides Prevention and Control

Huangtupo Landslide Demonstration Base

The Badong Huangtupo landslide demonstration base is located in the Huangtupo landslide area, which is the largest reservoir landslide by volume in TGRA (Tang et al. 2015a, b) (Fig. 17). This demonstration base is the largest underground landslide monitoring and testing facility in the world built to foster research, teaching, academic exchange on TGRA

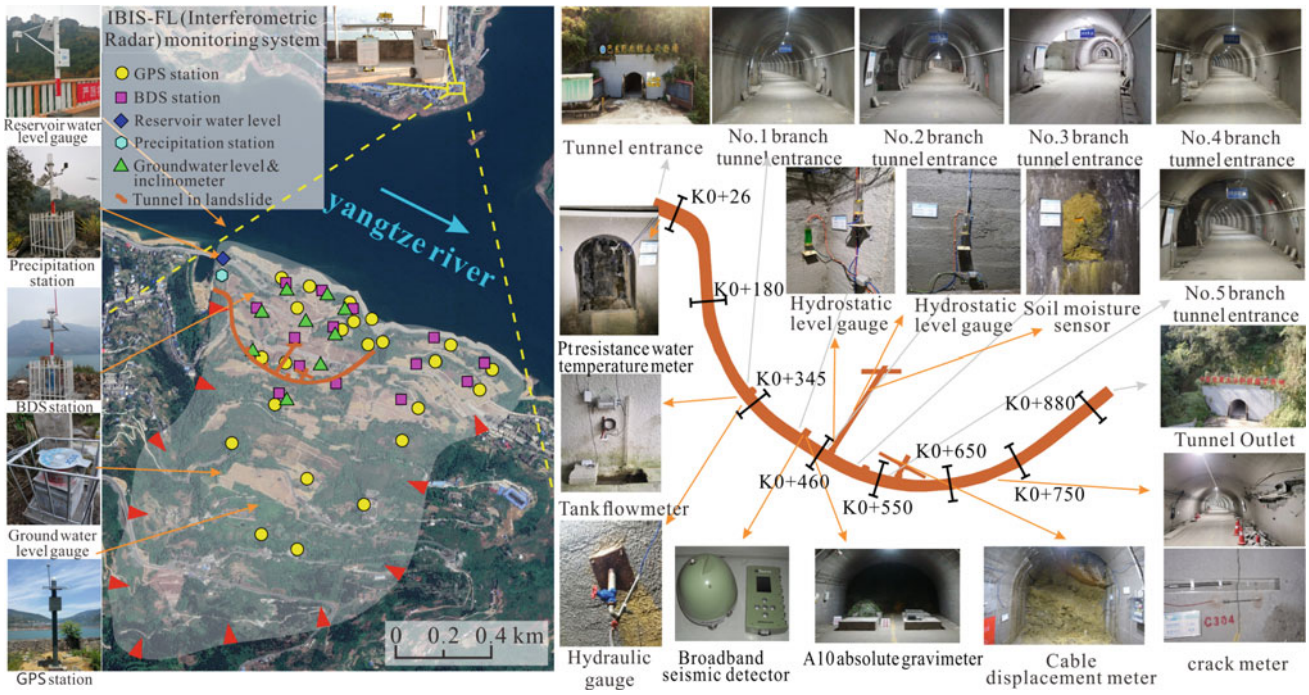

Fig. 17 Huangtupo landslide demonstration base (modified from Juang 2021)

geohazards. The station was designed and constructed and has been operated, by the China University of Geosciences since 2012. Over 10,000 people with a variety of geology-related backgrounds from >20 countries have visited this demonstration base.

The Huangtupo landslide demonstration base consists of a tunnel complex and a series of monitoring systems (Fig. 17). The tunnel complex, built in the Huangtupo riverside sliding mass #1, consists of a main tunnel with a length of 908 m and a width of 5 m, five branch tunnels (5–145 m long, 3.5 m wide), two test tunnels, and 35 observation windows. The test tunnels exposed the sliding zones of the landslide, facilitating their direct observation and the execution of scientific experiments, such as large-scale in-situ mechanical tests and deep deformation monitoring. The monitoring systems measure deformation as well as hydrologic, meteorological and hydro-chemical variables. The deformation system is composed of a slope surface displacement measurement unit and an underground displacement measurement unit. The slope surface displacement unit includes a number of GPS (Global Positioning System) and BDS (BeiDou Navigation Satellite System) measurement points, as well as an IBIS-FL (Interferometric Radar) monitoring system (Fig. 17). The underground displacement unit includes nine deep inclinometer boreholes, a number of crack meters installed on the ground and the walls of tunnels, and many hydrostatic level gauges that measure the settlement of the tunnels in the sliding mass. The hydrologic system includes a number of devices that allow for observation of the water level of the Yangtze River, the groundwater level, and water discharge of the tunnels (Fig. 17). A small meteorological station is located on the landslide and provides rainfall data. All these monitoring devices, except the inclinometers, have recently been updated with real-time acquisition and automatic transmission features (Tang et al. 2019).

In addition to the aforementioned monitoring system, the 3D deformation monitoring network techniques were also applied in the Huangtupo landslide demonstration base, including the flexible inclinometer (Zhang et al. 2018) and the pipeline trajectory inertial measurement instrument (Zhang et al. 2020).

The flexible inclinometer consists of a controller and a flexible inclinometer probe, of which, the length of the flexible inclinometer probe and the interval of the units can be customized depending on the specific application conditions before encapsulation (Fig. 18a). Encapsulated by silicone, the flexural rigidity of the flexible inclinometer probe can be ignored relative to the landslide mass, with displacement coupling well to the landside mass. With the advantages of good deformation coupling, large deformation capacity, and automatic measurement, the flexible inclinometer is suitable for continuous real-time monitoring of landslide deep displacement that undergoes multi evolutionary stages.

The pipeline trajectory inertial measurement instrument based on deformation-coupled pipeline trajectory measurement is deployed to fill the deficiencies of traditional

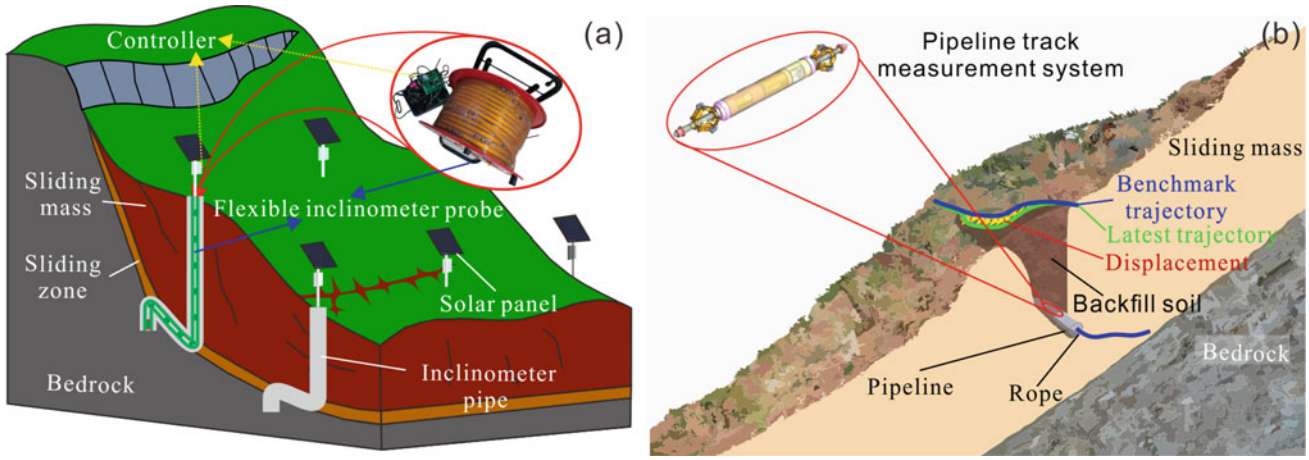

Fig. 18 3D deformation monitoring network techniques **a** the flexible inclinometer; **b** the pipeline trajectory inertial measurement instrument

instrumentation for measuring landslide displacement distributed along lateral direction (Fig. 18b). The developed instrument, primarily comprised of a single shaft gyro, two-axis accelerometers, and an external roller encoder, is designed to expediently calculate a pipeline trajectory with an Eulerian transformation when obtaining several basic physical variables, e.g., the axial linear velocity, pitch angle, roll angle, and azimuth angle. The pipeline trajectory inertial measurement instrument combined with pipeline and rope can be see as a pipeline track measurement system. With the pipeline trajectory measured at different times and compared with the benchmark trajectory, the pipeline track measurement system possesses the ability to reflect the displacement evolution feature of landslides. The results of prototype simulation tests imply a single measurement accuracy of a 12 cm/100 m span and a singly periodic multiple (more than five times) measurement accuracy of a 3 cm/100 m span, which meets medium-precision displacement measurement requirements for a landslide.

Majiagou Landslide Demonstration Base

The Majiagou landslide demonstration base is located in the Majiagou landslide in Zigui of TGRA. This demonstration base provides a platform to study the landslide stability during the reservoir operation, the interaction mechanism between the landslide and stabilizing structures, and the optimization design of stabilizing structures (Hu et al. 2017). An integrated, in-situ multi-parameter monitoring system was designed and installed during the test pile construction. The system included surface displacement and borehole monitoring, as well as experimental pile monitoring (Fig. 19). The surface deformation monitoring relied on five GPS stations and two fiber-sensing cables. The borehole monitoring system includes 15 boreholes, distributed along the main sliding direction, with different types of sensors installed to measure the deep displacement of the Majiagou landslide. The monitoring of the experimental piles (40 m long) relied on earth pressure gauges, stress gauges, strain gauges and fiber sensors. The earth pressure gauges were positioned on the surface of the piles to measure the lateral earth pressure. The stress gauges, strain gauges and strain-sensing fibers were installed in the stabilizing piles to measure the axial stress and the deflection of the piles. In each test pile, 26 stress gauges and strain gauges were installed to measure the longitudinal pile stress and strain. The thermo-sensing fibers were distributed along the experimental piles to monitor the change of temperature within the landslide.

7 Conclusions

This study introduced the recent advances in key techniques for reservoir landslide prevention and control based on evolutionary process.

The reservoir rock landslides can be divided into seven types based on the evolution modes, namely, progressive slip along gentle-dip layer I, progressive slip along gentle-dip layer II, bucking failure along steep-dip layer, creep slip along deep layer, plastic flow slip of weak interlayer, breakthrough abrupt slip in inclined cross-cutting layer and toppling failure in steep anti-dip layer, respectively. Then, according to the classification of the seven reservoir landslide evolution modes and corresponding evolution stages, the specific control measures suitable for reservoir landslides in different evolution stages are suggested and successfully employed in the management of Hongshibao landslide located in the TGRA.

A dynamic stability evaluation method is proposed considering the evolution process of the slip zone soil strength for the evaluation of landslide stability. This method is a

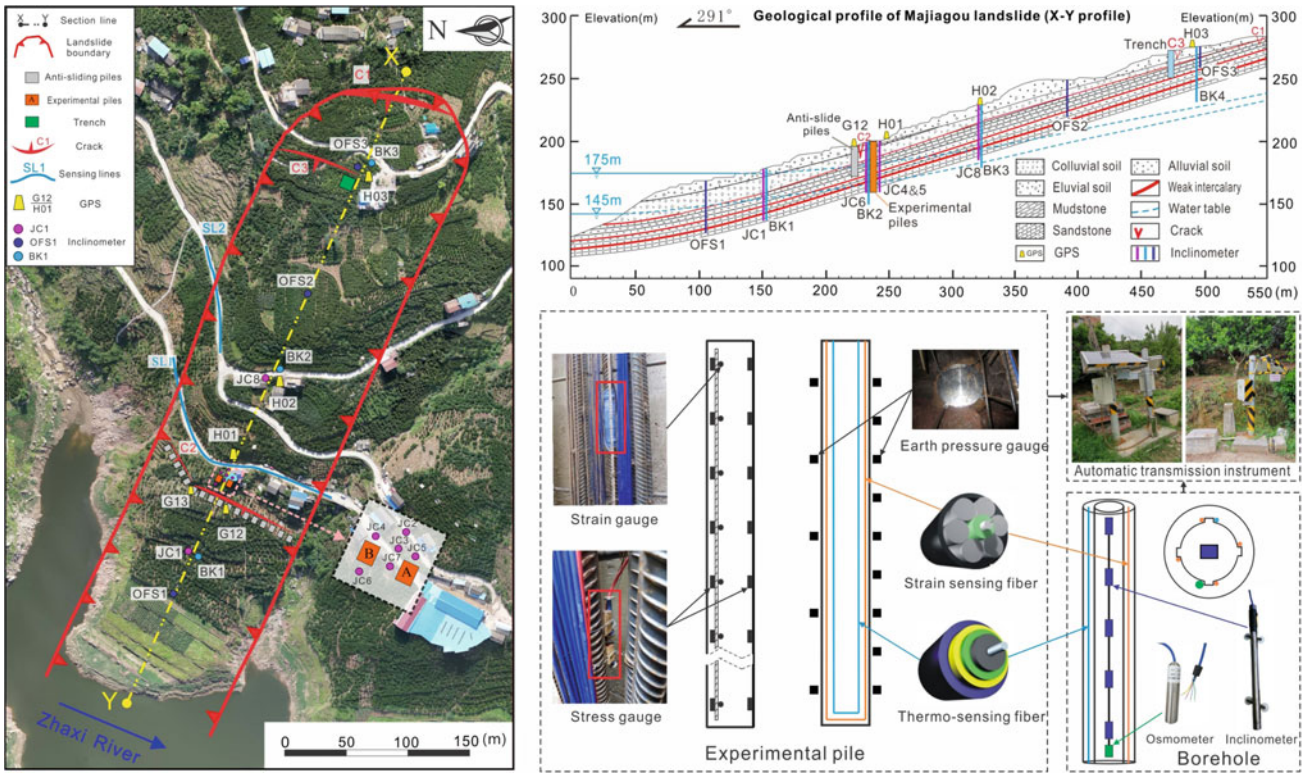

Fig. 19 Majiagou landslide demonstration base (Tang et al. 2019)

two-step regime: the constitutive model and shear strength evolution model for describing the relation between shear stress and shear displacement, and that between shear strength and shear displacement, respectively; and calculation of the stability factor as a function of the shear strength determined from the shear displacement of the slip zone soil. Then, we introduce three key techniques of reservoir landslide prevention and control: (1) determination of optimal pile position for step-shaped sliding surface, (2) the optimal plane arrangement method of stabilizing piles and (3) a reasonable embedded length determination method of stabilizing piles. In the first technique, we mainly address the actual sliding shapes rather than assuming an arc-shaped sliding surface, by adopting the so-called local safety partitioning (LSP) methodology. The second technique aims at solving the problem of unevenly distributed driving force that has not been properly addressed in conventional two-dimensional treatment. Further, the third technique gives the reasonable embedded length of piles in bedrock by incorporating the pile deformation into the supporting structure, which is important especially when complex layered bedrock is present.

Last, two demonstration bases for reservoir landslides prevention and control are introduced. The two demonstration bases with comprehensive monitoring system realize excellent applications of the new prevention and control techniques based on landslide evolution process, which can provide technical support for the landslide control of the same kind.

Acknowledgements The authors would like to express their sincere gratitude to the Ministry of Science and Technology of China and the National Natural Science Foundation of China (Nos: 42077268) for supporting this work.

References

Hu X, Tan F, Tang H, Zhang G, Su A, Xu C, Zhang Y, Xiong C (2017) In-situ monitoring platform and preliminary analysis of monitoring data of Majiagou landslide with stabilizing piles. Eng Geol 228:323–336

Juang CH (2021) BFTS-Engineering geologists' field station to study reservoir landslides. Eng Geol 284:106038

Li CD, Tang HM, Hu XL, Wang LQ (2013) Numerical modelling study of the load sharing law of anti-sliding piles based on the soil arching effect for Erliban landslide, China. KSCE J Civil Eng 17 (6):1251–1262

Li C, Wu J, Tang H, Wang J, Chen F, Liang D (2015) A novel optimal plane arrangement of stabilizing piles based on soil arching effect and stability limit for 3D colluvial landslides. Eng Geol 195:236–247

Li C, Yan J, Wu J, Lei G, Wang L, Zhang Y (2019) Determination of the embedded length of stabilizing piles in colluvial landslides with upper hard and lower weak bedrock based on the deformation control principle. Bull Eng Geol Env 78(2):1189–1208

Tan Q, Tang H, Huang L, Li C, Kou T (2018) LSP methodology for determining the optimal stabilizing pile location for step-shaped soil sliding. Eng Geol 232:56–67

Tang H, Li C, Hu X, Su A, Wang L, Wu Y, Criss R, Xiong C, Li Y (2015a) Evolution characteristics of the Huangtupo landslide based on in situ tunneling and monitoring. Landslides 12(3):511–521

Tang H, Li C, Hu X, Wang L, Criss R, Su A, Wu Y, Xiong C (2015b) Deformation response of the Huangtupo landslide to rainfall and the changing levels of the Three Gorges Reservoir. Bull Eng Geol Environ 74(3):933–942

Tang H, Wasowski J, Juang CH (2019) Geohazards in the three Gorges Reservoir Area, China—lessons learned from decades of research. Eng Geol 105267

Yan J, Zou Z, Mu R, Hu X, Zhang J, Zhang W, Su A, Wang J, Luo T (2022) Evaluating the stability of Outang landslide in the Three Gorges Reservoir area considering the mechanical behavior with large deformation of the slip zone. Nat Hazards

Zhang Y, Tang H, Li C, Lu G, Cai Y, Zhang J, Tan F (2018) Design and testing of a flexible inclinometer probe for model tests of landslide deep displacement measurement. Sensors 18(1):224

Zhang Y, Tang H, Lu G, Wang Y, Li C, Zhang J, An P, Sheng P (2020) Design and testing of inertial system for landslide displacement distribution measurement. Sensors 20(24):7154

Zhang J, Tang H, Tannant DD, Lin C, Xia D, Liu X, Zhang Y, Ma J (2021) Combined forecasting model with CEEMD-LCSS reconstruction and the ABC-SVR method for landslide displacement prediction. J Clean Prod 293:126205

Open Access This chapter is licensed under the terms of the Creative Commons Attribution 4.0 International License (http://creativecommons.org/licenses/by/4.0/), which permits use, sharing, adaptation, distribution and reproduction in any medium or format, as long as you give appropriate credit to the original author(s) and the source, provide a link to the Creative Commons license and indicate if changes were made.

The images or other third party material in this chapter are included in the chapter's Creative Commons license, unless indicated otherwise in a credit line to the material. If material is not included in the chapter's Creative Commons license and your intended use is not permitted by statutory regulation or exceeds the permitted use, you will need to obtain permission directly from the copyright holder.